Influence of the Anterolateral Ligament on Knee Laxity

A Biomechanical Cadaveric Study Measuring Knee Kinematics in 6 Degrees of Freedom Using Dynamic Radiostereometric Analysis

Emil Toft Nielsen,*†‡ MSc, Kasper Stentz-Olesen,† MSc, Sepp de Raedt,†§ MSc, PhD, Peter Bo Jørgensen,†‡ MSc, Ole Gade Sørensen,‖ MD, PhD, Bart Kaptein,¶ MSc, PhD, Michael Skipper Andersen,# MSc, PhD, and Maiken Stilling,†‡ MD, PhD

Investigation performed at the Department of Radiology and Orthopaedic Research Unit, Department of Orthopaedic Surgery, Aarhus University Hospital, Aarhus, Denmark

Background: An anterior cruciate ligament (ACL) rupture often occurs during rotational trauma to the knee and may be associated with damage to extracapsular knee rotation–stabilizing structures such as the anterolateral ligament (ALL).

Purpose: To investigate ex vivo knee laxity in 6 degrees of freedom with and without ALL reconstruction as a supplement to ACL reconstruction.

Study Design: Controlled laboratory study.

Methods: Cadaveric knees (N = 8) were analyzed using dynamic radiostereometry during a controlled pivotlike dynamic movement simulated by motorized knee flexion (0° to 60°) with 4-N·m internal rotation torque. We tested the cadaveric specimens in 5 successive ligament situations: intact, ACL lesion, ACL + ALL lesion, ACL reconstruction, and ACL + ALL reconstruction. Anatomic single-bundle reconstruction methods were used for both the ACL and the ALL, with a bone-tendon quadriceps autograft and gracilis tendon autograft, respectively. Three-dimensional kinematics and articular surface interactions were used to determine knee laxity.

Results: For the entire knee flexion motion, an ACL + ALL lesion increased the mean knee laxity ($P < .005$) for internal rotation (2.54°), anterior translation (1.68 mm), and varus rotation (0.53°). Augmented ALL reconstruction reduced knee laxity for anterior translation ($P = .003$) and varus rotation ($P = .047$) compared with ACL + ALL–deficient knees. Knees with ACL + ALL lesions had more internal rotation ($P < .001$) and anterior translation ($P < .045$) at knee flexion angles below 40° and 30°, respectively, compared with healthy knees. Combined ACL + ALL reconstruction did not completely restore native kinematics/laxity at flexion angles below 10° for anterior translation and below 20° for internal rotation ($P < .035$). ACL + ALL reconstruction was not found to overconstrain the knee joint.

Conclusion: Augmented ALL reconstruction with ACL reconstruction in a cadaveric setting reduces internal rotation, varus rotation, and anterior translation knee laxity similar to knee kinematics with intact ligaments, except at knee flexion angles between 0° and 20°.

Clinical Relevance: Patients with ACL injuries can potentially achieve better results with augmented ALL reconstruction along with ACL reconstruction than with stand-alone ACL reconstruction. Furthermore, dynamic radiostereometry provides the opportunity to examine clinical patients and compare the recontructed knee with the contralateral knee in 6 degrees of freedom.

Keywords: anterolateral ligament; anterior cruciate ligament; knee laxity; reconstruction; dynamic radiostereometric analysis; biomechanical analysis

Anterior cruciate ligament (ACL) reconstruction remains unable to replicate native knee kinematics.[50,62] Rotational knee laxity can lead to degenerative changes of the menisci and cartilage and eventually gonarthritis.[16,59] According to

The Orthopaedic Journal of Sports Medicine, 6(8), 2325967118789699
DOI: 10.1177/2325967118789699

Lohmander et al,[37] 50% of patients undergoing ACL reconstruction develop radiographic osteoarthritis within 2 decades of the injury.

Intra- and extra-articular knee-stabilizing surgical procedures have been studied.[13,51] Intra-articular reconstruction targets the ACL lesion, whereas the aim of extra-articular reconstruction is to reconstruct specific anatomic structures or the knee joint's functional anatomy. Recent years have seen renewed interest in the extra-articular lateral reinforcement concept to supplement intra-articular ACL reconstruction to reduce rotational laxity,[2,39,41] with particular attention being paid to the role of the anterolateral ligament (ALL) in relation to rotational laxity.

ALL research has focused on the anatomic bone attachment site and its association with the Segond fracture, which has been widely correlated with ACL injuries.[14,31,47,66] The cortical tibial avulsion site of the Segond fracture is equivalent to the tibial attachment of the ALL (midway between the Gerdy tubercle and the anterior border of the fibular head).[10,29] Thus, the presence of a Segond fracture could indicate an ALL rupture in patients with an ACL injury.[8,11] A radiographic examination can easily detect Segond fractures but will not detect soft tissue injuries. Furthermore, grading of the anterolateral structure is difficult, and arthroscopically nonaccessible ALL injuries may go unnoticed. Those patients who suffer from concurrent ACL and ALL injuries may therefore represent the group that harbors residual pivot-shift dysfunction after ACL reconstruction.[26]

Cadaveric studies have investigated the role of the ALL by determining changes in ligament length during knee flexion[14,20,71]; however, they report conflicting results possibly because they have used different definitions of the ALL's femoral origin.[9] Researchers largely agree on the tibial attachment site of the ALL but not on the femoral attachment site, which has been described as being anterior-distal[20,71] or posterior-proximal[14] to the fibular collateral ligament; moreover, variations of position and distinctness between patients have also been reported.[9,14,34] In a series of studies searching for the ideal and most isometric length-changing ALL reconstruction technique, different ALL attachment sites show different length-changing patterns during flexion.[25,28,30,33,42,67]

Other cadaveric studies have investigated the kinematic influence and/or force contribution of the ALL in intact, ACL-deficient, and/or ACL-reconstructed knees.[5,32,45,49,52,57,63,64] These studies have found that the ALL reduces knee laxity through passive restraint, but the extent to which laxity is restrained varies between studies. Most studies describe the ALL as a secondary restraint to internal rotation, with the ACL providing the primary restraint, but the ALL to some extent also restrains anterior translation.[5,45,49,52,57,63,64] The anterolateral restraining function of the ALL increases with increasing flexion angle.[45,49,63] Kittl et al[32] assigned only a minor role to the ALL compared with the iliotibial tract. They found that the ACL was the primary and the ALL the secondary contributor to knee laxity restraint at 30° to 90° of flexion. Additionally, cadaveric studies report diverging results when reconstructing the ALL; some report a potential for improving knee laxity compared with intra-articular ACL reconstruction,[43] whereas others show that ALL reconstruction does not restore native kinematics.[57] A recent study showed that ALL reconstruction overconstrains knee laxity.[52]

The role of the ALL in knee laxity has been extensively studied in recent years; however, laxity has mainly utilized static evaluation methods that do not mimic the dynamic pivot-shift–like[16] movement, which correlates with symptomatic functional instability.[1,36] Additionally, the preparation of the specimens in these cadaveric studies has generally encompassed removing the distal part of the thigh and the proximal part of the shank for fixing the bones in a robotic simulator and/or fully or partially dissecting the knee. The knee is a complex mechanical mechanism, and resecting superficial knee structures and fixating bone inevitably alter the native dynamics to some extent. Therefore, the ALL should be investigated in a setup that more resembles an in vivo human setting. Therefore, the purpose of this ex vivo study was to evaluate the contribution of the ALL to knee laxity in 6 degrees of freedom during a controlled pivotlike dynamic movement using dynamic radiostereometric recordings of full lower limb cadaveric specimens.

METHODS

Examinations were performed on 8 fresh-frozen human donor legs (from 2 female and 2 male patients) that included the foot, knee, and hemipelvis. A local ethical review board approved this study. The donors' age ranged from 58 to 94 years. The inclusion criteria were no known or surgically treated knee-associated fractures and no cruciate ligament or ALL lesions, which we assessed from the reported medical history, visual inspection for former surgical incisions, Lachman test, pivot-shift test, and radiographic inspection. Arthroscopic surgery was used during the experimental tests to verify the intactness of cruciate ligaments and meniscus.

*Address correspondence to Emil Toft Nielsen, MSc, Orthopaedic Research Unit, Department of Orthopaedic Surgery, Aarhus University Hospital, Palle Juul-Jensens Boulevard 99, Entrance J, Aarhus, Denmark (email: emiltn@clin.au.dk).
†Orthopaedic Research Unit, Department of Orthopaedic Surgery, Aarhus University Hospital, Aarhus, Denmark.
‡Department of Clinical Medicine, Aarhus University, Aarhus, Denmark.
§NRT X-RAY A/S, Hasselager, Denmark.
‖Department of Sports Traumatology, Aarhus University Hospital, Aarhus, Denmark.
¶Biomechanics and Imaging Group, Department of Orthopaedic Surgery, Leiden University Medical Center, Leiden, the Netherlands.
#Department of Materials and Production, Aalborg University, Aalborg, Denmark.
The authors declared that they have no conflicts of interest in the authorship and publication of this contribution.
Ethical approval for this study was waived by the Central Denmark Regional Committee on Health Research Ethics.

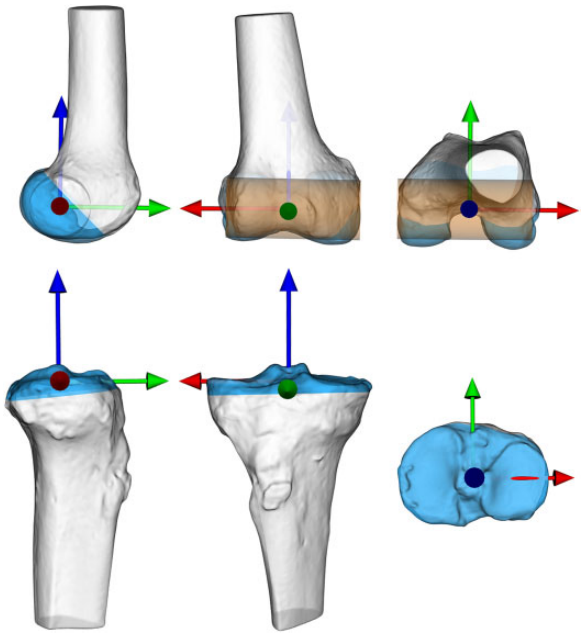

Figure 1. Computed tomography bone models of the femur (top) and tibia (bottom) illustrated along each axis of the anatomic coordinate system for a right leg (red pointing lateral, green pointing anterior, and blue pointing proximal). From left, a lateral, anterior, and proximal view. The lateral-medial axis was defined by an orthogonal projection of the mechanical axis to the center line of a cylinder (cupper), which was positioned using a least-squares fit to the condyles (blue area). The midpoint between the lateral and medial intersections of the lateral-medial axis and bone model surface was assigned as the origin. The proximal-distal axis was determined as the fixed mechanical axis between the femoral origin and the center of a sphere fitted to the femoral head using a least-squares fit. The cross-product of the proximal-distal and lateral-medial axes defined the anterior-posterior axis. The origin of the tibial coordinate system was defined by the centroid of the tibial plateau (blue area), which was cut off at the largest cross section. The proximal-distal axis was defined as the mechanical axis between the tibial origin and the center of the tibial articular surface in the ankle joint. The lateral-medial axis was defined by an orthogonal projection of the mechanical axis to the first principal component of the tibial plateau (blue area). The cross product of the proximal-distal and lateral-medial axes defined the anterior-posterior axis.

The knee joints of the intact frozen specimens were scanned with a clinical computed tomography (CT) scanner (Brilliance 40; Philips) using axial slices at 120 kVp and 150 mAs, slice thickness of 0.9 mm, slice increment of 0.45 mm, and pixel size of 0.39 × 0.39 mm. A fully automated method[12,35] using graph cuts for segmentation of the 3-dimensional CT volumes was used to generate 8 CT bone models of the femur and tibia. These models (Figure 1) covered the distal 15 cm of the femur and proximal 15 cm of the tibia. Each segmented bone model was remeshed from approximately 500,000 to 10,000 triangular elements. Each generated CT bone model was assigned to a local anatomic coordinate system (ACS) using a fully automated method,[40] except that we used the mechanical axis as the proximal-distal axis.

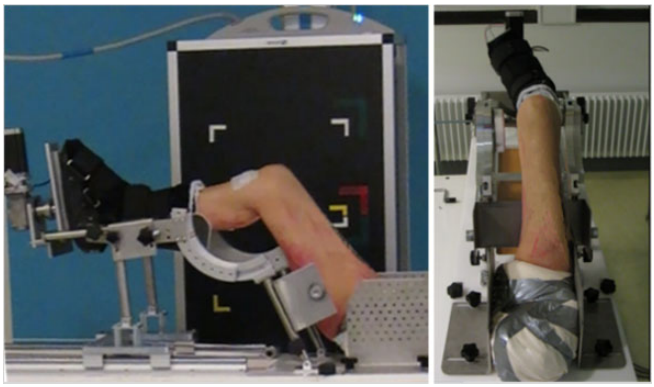

Figure 2. Lateral sagittal (left) and distal-proximal (right) views of the motorized fixture with a right leg installed.

Experimental Setup and Equipment

A customized, motorized fixture (Figure 2) was built to support the thigh and lower leg, and the knee area was kept completely uncovered to avoid image artifacts. The hemipelvis was fixed to the base of the apparatus using 3 regular screws at the sacrum, iliac crest, and pubic bone. The foot and ankle joints were fixed in 90° of ankle flexion using a Pro+ Fixed Walker (VQ OrthoCare). The boot shaft was shortened by approximately 10 cm. A stepper motor (3 N·m) (NEMA 23; National Instruments) was installed with pulley wheels, a timing belt, and 2 linear sliders to perform controlled dynamic knee motion from approximately 0° to 100° of flexion and back at a rate of 0.1 m/s. Another NEMA 23 motor was mounted to the footrest to control internal rotation. A slow speed (0.001 m/s) enabled manual stop of the motor when the desired torque of 4 N·m was reached in the fully extended knee. The torque was measured using a torque sensor (accuracy, ±0.15%; repeatability, ±0.03%) (TQ 201-500; OMEGA) and an adjacent meter (DP25B-S-230; OMEGA). Both motors were controlled using a driver (DM542A; Longs Motor) and a breakout board (DB25; Sunwin).

Stereoradiographs were recorded using dynamic radiostereometric analysis (dRSA) (Adora RSAd; Nordisk Røntgen Teknik) with a 10-Hz sampling frequency. A vertically placed uniplanar calibration box (Box 14; Medis Specials) and a vertical tube setup (16° tube angles) were used to maximize visualization of the knee joint line during motion. The full detector size of 37 (horizontal) × 42 cm was used to record knee motion from 0° to 60° of flexion. The source-image distance was 2.94 m, and the focus-skin distance was 2.38 m. Exposure settings for dynamic recordings were 90 kV, 500 mA, and 2.5 milliseconds, with a resolution of 1104 × 1344 pixels (79 DPI).

Test Protocol

At 72 hours before testing, specimens were thawed at 5°C. Each specimen underwent 5 series of identical tests. One

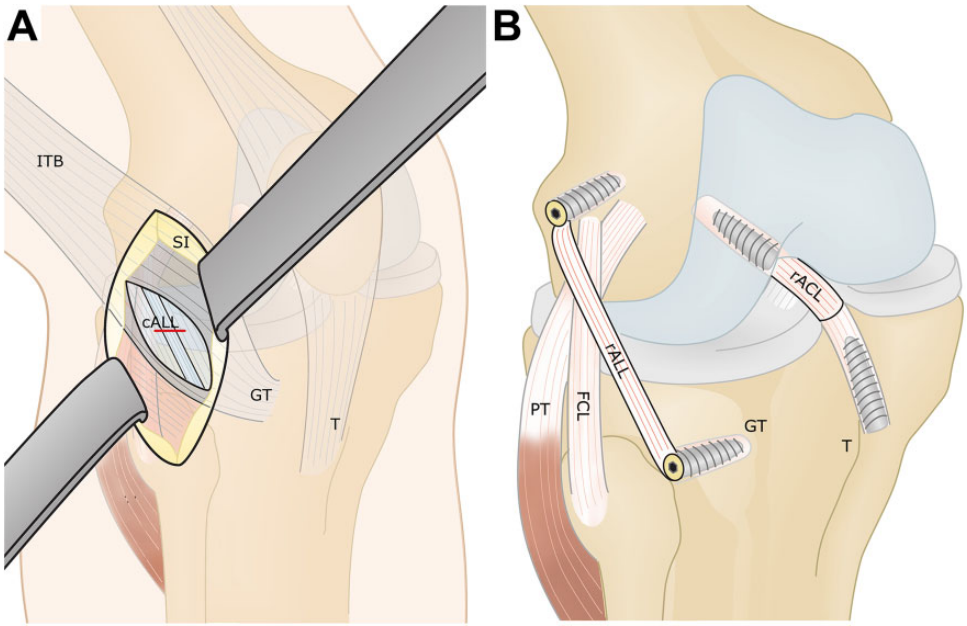

Figure 3. (A) Illustration of the access and cutting of the anterolateral ligament (ALL). (B) Illustration of the 2 reconstruction methods of the anterior cruciate ligament (rACL) and ALL (rALL). cALL, cut ALL; FCL, fibular collateral ligament; GT, Gerdy tubercle; ITB, iliotibial band; SI, skin incision; T, tuberosity.

series of tests assessed 1 ligament situation. Each series consisted of 1 machine-controlled test and 3 manual tests. First, each specimen was carefully fixed to the machine, and a motor-driven pivotlike maneuver was simulated by applying constant internal rotation (4 N·m of torque during full knee extension) to the foot and lower leg at motion initialization. This rotation was maintained during knee flexion (0° to 100°). Subsequently, manual tests were conducted by an experienced knee surgeon (O.G.S.) in a manner similar to that used in clinical practice.[6] The anteroposterior translation laxity of the tibia was measured using the Lachman test (grade, 0-3)[65] and the mean of 3 Rolimeter tests (mm).[4] Rotational laxity was determined using the mean of 3 pivot-shift tests (grade, 0-3).[16]

The same experienced surgeon conducted all surgical procedures. The order of the tested ligament situations was consistent for all specimens. The first series of tests was conducted with an intact knee. Subsequently, the ACL was resected (cACL), and then the ALL was cut (cACL-cALL). These procedures were followed by reconstruction of the ACL (rACLcALL) and then the ALL (rACLrALL). The ACL was visualized during arthroscopic surgery in all specimens after the first series of tests and was then removed with a shaver before the second series of tests. The ALL was accessed through a vertical skin incision from the lateral femoral epicondyle to midway between the Gerdy tubercle and the fibular head. The iliotibial tract was divided longitudinally at the joint level. Next, ALL fibers including the capsule were cut with a 2-cm horizontal incision approximately 1 cm proximal to the tibial attachment site (Figure 3A). The iliotibial tract was closed with a Vicryl 2-0 suture (Ethicon) before the next test series. Single-bundle anatomic ACL reconstruction was performed using a bone-tendon quadriceps autograft with a 9-mm diameter. The articular entry point of the bone tunnel in the femur and tibia was placed according to anatomic studies performed by Śmigielski et al[55] and Siebold et al.[54] The ACL was fixed with a 7 × 25–mm Biosure interference screw (Smith & Nephew) in the femur and a 9 × 25–mm Biosure interference screw in the tibia. Anatomic single-bundle reconstruction of the ALL with a gracilis tendon autograft was performed as described by Sonnery-Cottet et al[56] with minor changes. The only difference between the methods involved tibial graft fixation. Instead of looping the graft in the tibia, the single-bundle graft was fixed with a screw midway between the Gerdy tubercle and the fibular head, 1 cm inferior to the joint line. The femoral attachment site was placed approximately 8 mm proximally and posteriorly to the lateral femoral epicondyle. A 6 × 25–mm Biosure interference screw was used for both femoral and tibial fixation of the ALL graft. The graft was tensioned and fixed in 10° to 20° of flexion (Figure 3B).

Radiographic Analysis

The dynamic stereoradiographs were analyzed using commercially available software (Model-Based RSA v 4.02; RSAcore).[58] The fitting process of the CT bone model to the radiographs was performed meticulously using as many contours (external and internal) of the bone in all directions as possible (Figure 4). The included contours for the femur were the shaft, condyles, and supracondylar line. For the tibia, the included contours were the shaft, eminencies, and medial and lateral plateaus. Because of the confined recording area, only knee angles between 0° and 60° of flexion contained enough of the tibial and femoral bone on the

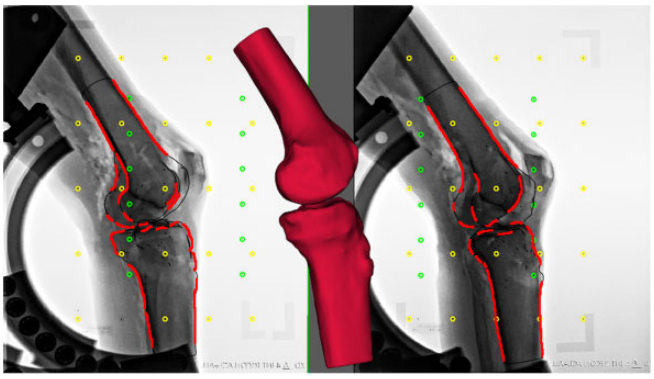

Figure 4. A radiographic image illustrating a computed tomography (CT) bone model pose optimized by minimizing the matching error between the virtual CT bone model projection (black edges) and the actual projections detected (red edges) in the radiographs. The matching error is the mean distance (in mm) between the CT bone model surface and the projection lines that connect the X-ray focus with the detected edges in the radiographs. The contours are enhanced in the image for better visualization. The fiducial (yellow) and control (green) marker sets of the calibration box are illustrated.

stereoradiographs to be analyzed. Three model-optimization algorithms (IIPM, DIFDoNLP, and DIFDHsAnn) from Model-Based RSA software were used successively to optimize the CT bone model pose (position and orientation) on the radiographic projection.[27,48]

Data Processing and Statistical Analysis

Customized software (MATLAB R2015b; MathWorks) was developed to investigate the biomechanical effect of the ALL. The raw kinematic data from the Model-Based RSA analysis (n = 624) describing the anatomic linear and angular movements of the femur and tibia included approximately every 2.5° to 5° of knee flexion. For illustrations and comparisons between specimens, measures of anatomic displacement and rotation, as well as contact points at the tibia, were linearly interpolated with knee flexion angle increments of 2.5°.

To ensure clinical relevance, the anatomic displacements and rotations of the knee were standardized in accordance with terms introduced by Grood and Suntay.[17] The contact points during the dynamic interaction between the femoral condyles and tibial plateau were determined in accordance with Anderst and Tashman,[3] with 1 significant modification: Instead of using the tibial plateau of the bone model, a tibial transverse plane intersecting the tibial origin was defined by the anterior-posterior and lateral-medial axes to avoid detecting tibial eminences as a contact point between the tibia and femur.

The femoral contact point was estimated by the weighted-average method used by Anderst and Tashman.[3] Briefly, the centroids of each triangular element of the femur were weighted based on their proximity to the defined tibial transverse plane. The estimated tibial contact point was identified by projecting the contact point at the femur to the tibial plane along the tibial proximal-distal axis. To achieve the most accurate estimate of contact points, the 8 high-resolution original bone models (before remeshing) were used.

To further investigate the nature of the contact points, we adopted the approach of Hoshino and Tashman.[22] These authors reported that the path length of the contact points offers further insights into the dynamic interaction between the tibia and femur. The femoral path length was estimated as the sum of the sagittal excursion between contact points. The tibial path length was estimated as the sum of the transverse-plane length between contact points. The lateral and medial sliding lengths (sliding) were estimated by the difference between the path lengths of the femoral and tibial contact points. The difference in sliding was also calculated as the difference between the lateral and medial sliding lengths.

The kinematic data and path length calculations are presented as absolute and normalized values. Absolute values were estimated directly with no further processing. Normalized values were determined by subtracting observations for each ligament situation by observations for intact knees. This normalization removes idiosyncratic variations across individual specimens.

All statistical analyses were conducted using Stata 14 (StataCorp). A mixed model was used on the measures of kinematic translation and rotation as well as the contact point excursion analysis to take into account repeated measurements on the cadaveric specimens, pairs, and ligament situations. Model validation was performed by visually inspecting residuals, fitted values, and random-effect estimates. The Wald test was used to analyze the systematic difference. A similar mixed-model method was used for the anterior and posterior Rolimeter tests; however, for the nonparametric Lachman and pivot-shift tests, model validation was unacceptable because of nonnormally distributed residuals and random-effect estimates. Because a nonparametric test is likely to be more robust than a mixed model, the Wilcoxon signed-rank test was performed for the Lachman and pivot-shift tests. A significance level of .05 was used for all tests.

RESULTS

The tibiofemoral joint kinematics with respect to flexion angle are illustrated in Figure 5 for all 5 ligament situations and all 5 degrees of freedom: varus-valgus rotation, external-internal rotation, lateral-medial translation, anterior-posterior translation, and proximal-distal translation.

Kinematic Analysis

Figure 6 illustrates the normalized values of each ligament situation. Throughout the motion, larger internal rotation (Δ1.76°-2.48°, $P < .01$) and anterior translation (Δ0.62-1.53 mm, $P < .05$) were observed for all ligament situations compared with ligament-intact knees. Anterior

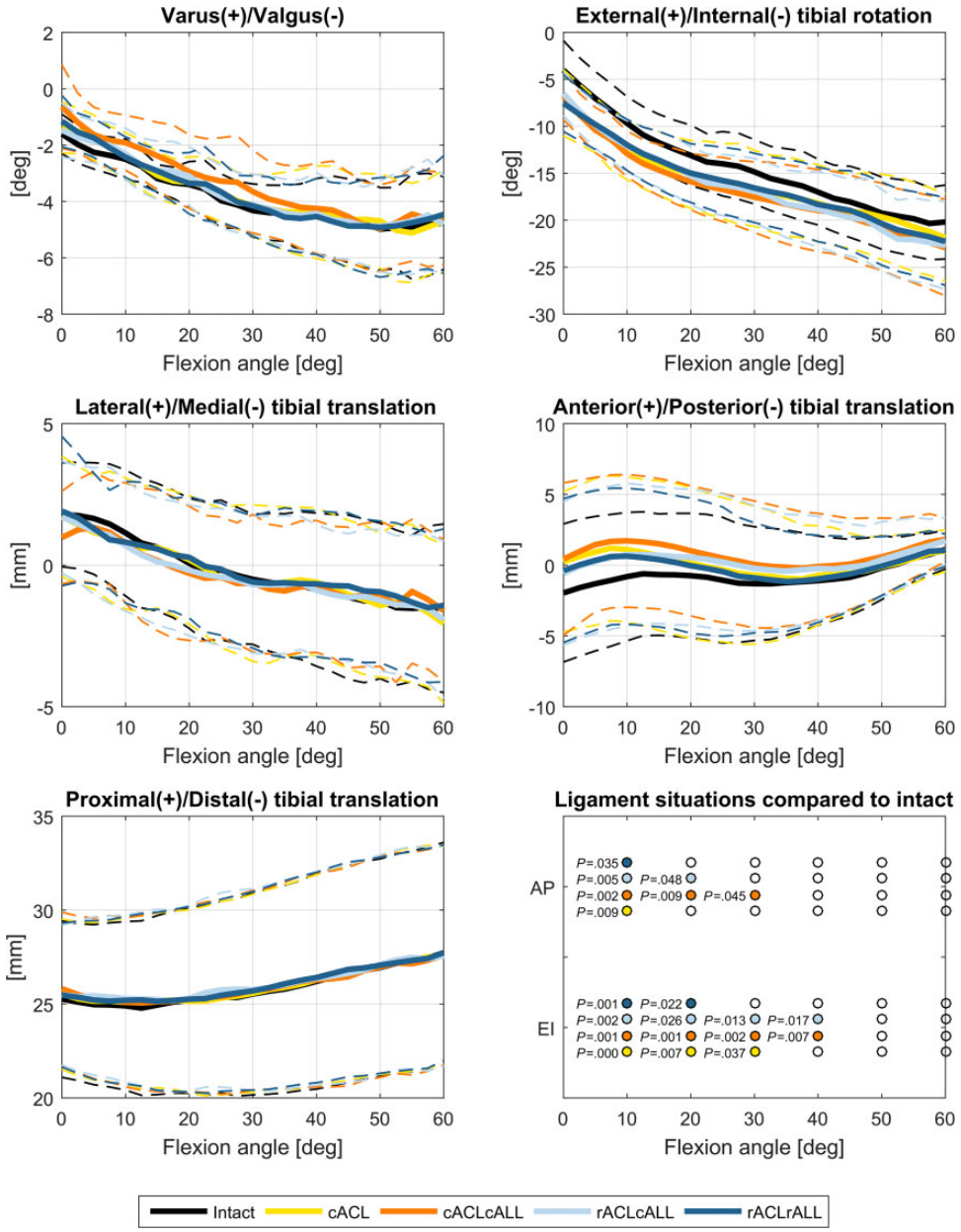

Figure 5. The kinematics of the tibiofemoral joint during knee flexion from 0° to 50° for all ligament situations. The 5 degrees of freedom included varus-valgus rotation, external-internal (EI) rotation, lateral-medial translation, anterior-posterior (AP) translation, and proximal-distal translation. The solid lines represent the mean, and the dashed lines represent the 95% CI of the mean. The subplot in the bottom right illustrates, by the colored dots, which ligament situations are significantly different from the intact knee at knee flexion angles grouped in ranges of 10° for all 5 degrees of freedom. The corresponding *P* value is listed to the left of the colored dot. ACL, anterior cruciate ligament; ALL, anterolateral ligament; cACL, cut ACL; cACLcALL, cut ACL and then cut ALL; rACLcALL, cut ALL and then reconstruction of the ACL; rACLrALL, reconstruction of the ACL and then reconstruction of the ALL.

translation was also larger for the cACLcALL knees than with cACL (Δ0.70 mm, $P < .03$) and less for the rACLrALL knees compared with cACLcALL (Δ0.91 mm, $P < .01$). Varus rotation was larger for cACLcALL than for the intact condition (Δ0.46°, $P < .01$) and was also less for the rACLrALL knees compared with cACLcALL (Δ0.33 mm, $P < .01$). For lateral-medial translation and proximal-distal translation, none of the ligament situations was significantly different from the intact knee. However, less medial translation was found with the rACLrALL knees than with cACLcALL (Δ0.21 mm; $P < .05$) or rACLcALL (Δ0.21 mm; $P = .03$).

Further inspection of anterior-posterior translation and external-internal rotation showed that the differences

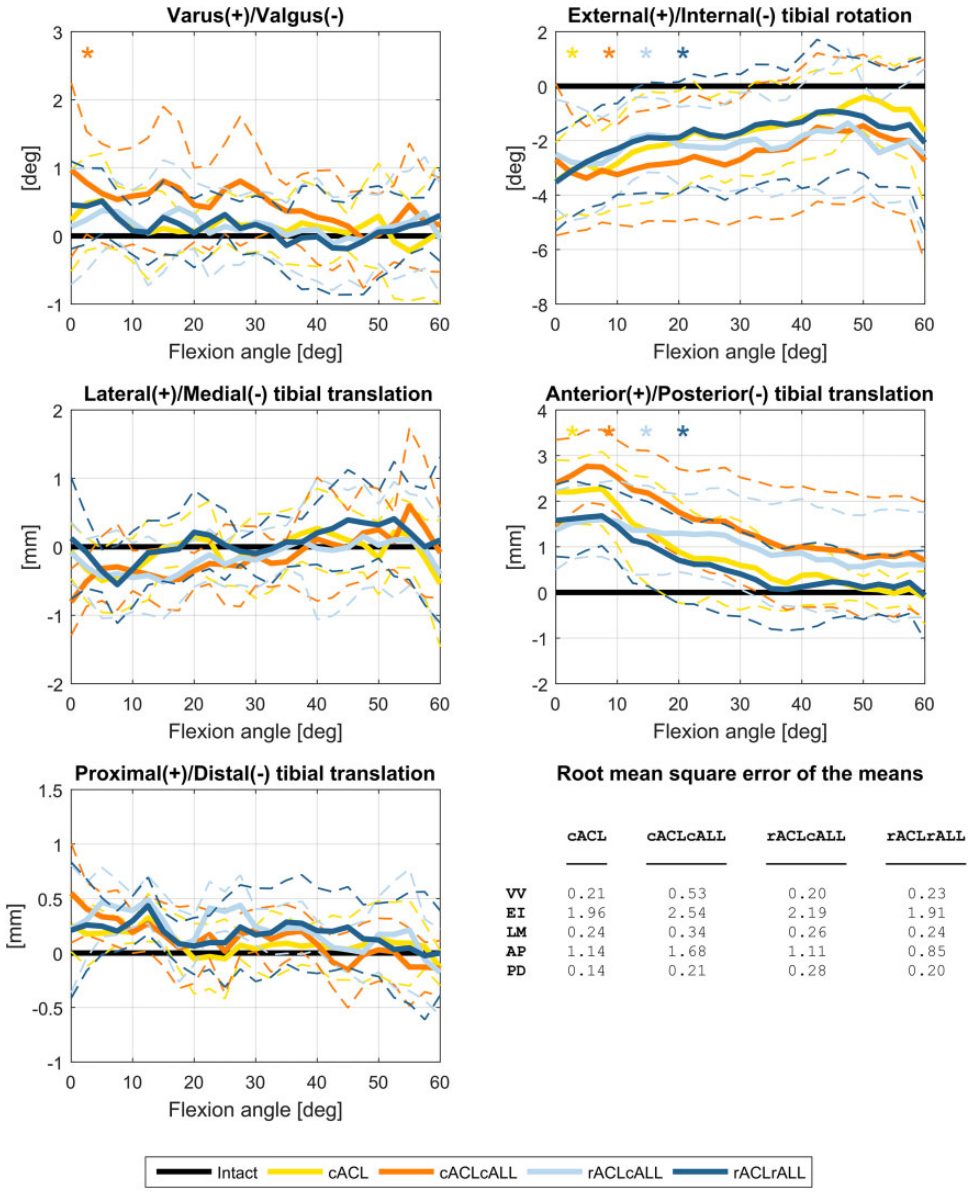

	cACL	cACLcALL	rACLcALL	rACLrALL
VV	0.21	0.53	0.20	0.23
EI	1.96	2.54	2.19	1.91
LM	0.24	0.34	0.26	0.24
AP	1.14	1.68	1.11	0.85
PD	0.14	0.21	0.28	0.20

Figure 6. The normalized kinematics of the tibiofemoral joint during knee flexion from 0° to 50° for all ligament situations. The 5 degrees of freedom included varus-valgus (VV) rotation, external-internal (EI) rotation, lateral-medial (LM) translation, anterior-posterior (AP) translation, and proximal-distal (PD) translation. The solid lines represent the mean, and the dashed lines represent the 95% CI of the mean. The stars in the top left of the subplot indicate that the respective ligament situation is significantly different from the intact knee throughout the entire motion. The subplot at the bottom right shows the root mean square of the means of each ligament situation compared with the intact knee. ACL, anterior cruciate ligament; ALL, anterolateral ligament; cACL, cut ACL; cACLcALL, cut ACL and then cut ALL; rACLcALL, cut ALL and then reconstruction of the ACL; rACLrALL, reconstruction of the ACL and then reconstruction of the ALL.

between the intact knee and the other ligament situations were largest at small flexion angles, and they were reduced as knee flexion angles increased. Figure 5 illustrates which ligament situations were significantly different from the intact knee at varying flexion angles. Flexion angles were grouped in 10° increments.

For external-internal rotation, the cACL knees ($P < .04$) had larger internal rotation than the intact knees at flexion angles ranging from extension (Δ3.1° [95% CI, 4.9°-1.4°]) to 30° (Δ1.9° [95% CI, 3.6°-0.1°]). The cACLcALL ($P < .01$) and rACLcALL ($P < .03$) knees had larger internal rotation than the intact knees at flexion angles ranging from extension (Δ3.1° [95% CI, 4.8°-1.3°] and Δ2.7° [95% CI, 4.5°-1.0°], respectively) to 40° (Δ2.4° [95% CI, 4.2°-0.7°] and Δ2.1° [95% CI, 3.9°-0.4°], respectively). Compared with the intact knee, the rACLrALL knee ($P < .02$) was the only construct

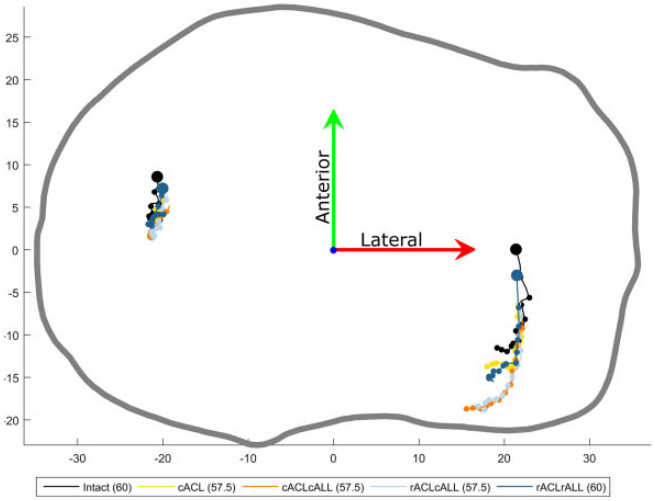

Figure 7. The contact path length was determined by estimating the articular surface interaction between the femur and tibia. The thin solid lines represent the path of the contact points that begin at the large dot (0° of knee flexion). Subsequently, each dot represents increments of 5° of knee flexion. The thick solid gray line represents the tibial perimeter of the largest cross section of the anterior-posterior and lateral-medial planes. The anatomic coordinate system is illustrated in green (anterior-posterior axis) and red (lateral-medial axis) and is connected by a blue dot (origin). ACL, anterior cruciate ligament; ALL, anterolateral ligament; cACL, cut ACL; cACLcALL, cut ACL and then cut ALL; rACLcALL, cut ALL and then reconstruction of the ACL; rACLrALL, reconstruction of the ACL and then reconstruction of the ALL.

with larger internal rotation at 0° to 20° of flexion. The mean difference was seen at extension (3.0° [95% CI, 4.2°-0.7°]) and at 20° of flexion (2.0° [95% CI, 3.8°-0.3°]).

For anterior-posterior translation, the cACL ($P = .009$) and rACLrALL ($P = .035$) knees had larger anterior translation at 0° to 10° of flexion than the intact knee, with a mean difference of 2.2 mm (95% CI, 0.6-3.9) and 1.6 mm (95% CI, 0.1-3.1), respectively. The cACLcALL knees ($P < .045$) had larger anterior translation than the intact knee at flexion angles ranging from extension (Δ2.6 mm [95% CI, 1.0-4.3]) to 30° (Δ1.6 mm [95% CI, 0.1-3.1]). The rACLcALL knees ($P < .05$) had larger anterior translation than the intact knee at flexion angles ranging from extension (Δ1.6 mm [95% CI, 0.1-3.1]) to 30° (Δ1.5 mm [95% CI, 0.0-3.0]).

For varus-valgus rotation, lateral-medial translation, and proximal-distal translation, none of the ligament situations was found to be significantly different from the intact knee in 10° ranges.

Contact Path Analysis

The contact path had a relatively constant medial contact point, whereas the lateral contact point moved posteriorly and slightly medially during knee flexion. However, for the majority of the specimens, the first lateral contact point for the intact knee was clearly positioned anteriorly to the first lateral contact point for all other ligament situations. The ligament situation with the contact point nearest to the contact point of the intact knee was rACLrALL in 50% of the specimens. For the remaining specimens, no clear pattern was observed. Figure 7 illustrates an example in which the contact path did not change until the ALL was cut. Likewise, a return to the contact path of the intact knee was not observed until the ALL was reconstructed. Resection of the ALL caused posterior displacement at the end of the contact path with a slight delay of the subsequent medial movement.

Table 1 shows the estimated femoral and tibial contact path excursions in the lateral and medial compartments. The actual and normalized distances are shown with their corresponding *P* values.

Manual Testing

Results of the manual tests (Lachman, anterior Rolimeter, posterior Rolimeter, and pivot-shift) revealed differences in knee laxity between ligament situations (Table 2). In all 4 manual tests, the largest differences were found when resecting and reconstructing the ACL ($P < .02$), while only minor differences were found when resecting and reconstructing the ALL ($P < .02$). Compared with the intact knee, the laxity of the cACL knees increased in all tests ($P < .02$); however, the cACLcALL knees were only different from the cACL knees for the anterior Rolimeter and pivot-shift tests ($P < .01$).

For all tests, the rACLcALL situation decreased knee laxity compared with the cACL and cACLcALL situations ($P < .02$). Only the pivot-shift test showed larger laxity ($P < .015$) for the rACLcALL knees than for the intact knee. In addition, results of the pivot-shift test showed decreased knee laxity from the the rACLcALL to the rACLrALL situation.

DISCUSSION

The most important findings of this ex vivo study were that ALL resection increased knee laxity in ACL-deficient knees and that ALL reconstruction in ACL-reconstructed knees approached native knee laxity during simulated movements such as the pivot shift using full lower limbs.

The largest effects of ALL resection were found during external-internal and anterior-posterior movements. The evaluation of knee laxity at 10° increments of knee flexion revealed that the rACLrALL situation was not significantly different from the intact knee above 10° for anterior-posterior translation. For external-internal rotation, no significant differences were found above 20°. In contrast, the cACLcALL situation was significantly different from the intact knee at knee flexion below 40°. Interestingly, ACL reconstruction did not reduce knee laxity for external-internal rotation until the ALL was also reconstructed. Thus, our study demonstrates that ALL-reconstructed knees resemble intact knees at flexion angles (30°-40°) in which giving way occurs in ACL-deficient knees, for

TABLE 1
Contact Path Excursion of the Femur and Tibia in the 5 Ligament Combinations During Knee Flexion From 0° to 50°[a]

	Intact	cACL			cACLcALL			rACLcALL			rACLrALL		
	Absolute	Absolute	Normalized	*P*	Absolute	Normalized	*P*	Absolute	Normalized	*P*	Absolute	Normalized	*P*
Lateral													
Femur	26.6 ± 6.0	26.5 ± 6.0	–0.1 ± 0.1	.33	26.4 ± 5.8	–0.2 ± 0.2	.20	26.3 ± 6.3	–0.4 ± 0.2	.06	26.6 ± 6.0	0.0 ± 0.0	.75
Tibia	23.0 ± 5.9	20.7 ± 5.4	–2.7 ± 0.7	.00[b]	21.3 ± 6.2	–1.6 ± 0.6	.07[b]	20.6 ± 4.0	–2.4 ± 1.0	.01[b]	19.4 ± 3.9	–3.6 ± 1.0	.00[b]
Sliding	3.6 ± 10.5	6.2 ± 9.2	2.6 ± 0.7	.00[b]	5.0 ± 10.4	1.4 ± 0.7	.03[b]	5.7 ± 9.8	2.0 ± 1.1	.06	7.2 ± 8.1	3.6 ± 0.9	.00[b]
Medial													
Femur	29.4 ± 4.7	29.2 ± 4.5	–0.2 ± 0.2	.27	29.3 ± 5.0	–0.1 ± 0.3	.60	29.1 ± 4.7	–0.3 ± 0.2	.11	29.6 ± 5.1	0.2 ± 0.2	.37
Tibia	13.0 ± 4.8	12.4 ± 4.4	–0.6 ± 1.0	.52	13.4 ± 4.8	0.4 ± 0.8	.61	13.1 ± 4.7	0.0 ± 0.6	.96	12.3 ± 4.7	–0.7 ± 0.9	.42
Sliding	16.4 ± 5.3	16.8 ± 6.6	0.5 ± 1.0	.65	15.8 ± 6.0	–0.5 ± 0.7	.45	16.1 ± 5.5	–0.3 ± 0.6	.61	17.3 ± 5.4	0.9 ± 0.5	.05
Δ Sliding	12.7 ± 10.1	10.6 ± 10.5	–2.1 ± 1.0	.03[b]	10.8 ± 9.6	–1.9 ± 0.9	.03[b]	10.4 ± 10.9	–2.3 ± 1.3	.06	10.1 ± 8.2	–2.7 ± 1.1	.01[b]

[a]Values are shown as mean ± SD (in mm). The absolute and normalized (to intact) values are shown. The *P* value for each ligament combination refers to the comparison with the intact ligament combination. Δ Sliding refers to difference between the medial and lateral sliding. ACL, anterior cruciate ligament; ALL, anterolateral ligament; cACL, cut ACL; cACLcALL, cut ACL and then cut ALL; rACLcALL, cut ALL and then reconstruction of the ACL; rACLrALL, reconstruction of the ACL and then reconstruction of the ALL.
[b]$P < .05$.

TABLE 2
Results of the Rolimeter, Pivot-Shift, and Lachman Manual Tests for Each Ligament Combination[a]

	Intact	cACL	cACLcALL	rACLcALL	rACLrALL
Anterior Rolimeter test, mm	4.0 ± 1.2	7.6 ± 2.0[b]	9.4 ± 1.4[b,c]	4.5 ± 1.1[c,d]	4.4 ± 0.7[c,d]
ΔAnterior Rolimeter test, mm		3.6 ± 2.1	5.3 ± 2.0	0.4 ± 1.5	0.3 ± 1.1
Posterior Rolimeter test, mm	3.4 ± 0.6	5.8 ± 1.3[b]	5.3 ± 0.9[b]	3.4 ± 0.8[c,d]	3.2 ± 0.9[c,d]
ΔPosterior Rolimeter test, mm		2.4 ± 1.3	2.0 ± 0.8	0.1 ± 1.1	0.1 ± 1.3
Pivot-shift test (grade, 0-3)	0.0 ± 0.0	1.2 ± 0.4[b]	1.8 ± 0.8[b,c]	0.2 ± 0.4[c,d,e]	0.0 ± 0.0[c,d,f]
Lachman test (grade, 0-3)	0.0 ± 0.0	2.8 ± 0.5[e]	2.9 ± 0.4[e]	0.3 ± 0.5[g,h]	0.1 ± 0.4[g,h]

[a]Values are shown as mean ± SD. Δ indicates the difference to intact. All ligament situations were compared for significant differences within each test type. ACL, anterior cruciate ligament; ALL, anterolateral ligament; cACL, cut ACL; cACLcALL, cut ACL and then cut ALL; rACLcALL, cut ALL and then reconstruction of the ACL; rACLrALL, reconstruction of the ACL and then reconstruction of the ALL.
[b]Intact ($P < .0001$).
[c]cACL ($P < .0001$).
[d]cACLcALL ($P < .0001$).
[e]Intact ($P < .015$).
[f]rACLcACL ($P < .003$).
[g]cACL ($P < .015$).
[h]cACLcALL ($P < .015$).

example during combined stepping and crossover cutting tasks[24] and stepping-down tasks.[23] These knee angles are used when performing a manual pivot-shift test; indeed, we found coherence between knee laxity during dRSA in this knee flexion range and the manual pivot-shift test. This suggests that clinically, patients with significant anterolateral laxity may have ALL damage and could potentially benefit from ALL reconstruction. Of all manual tests, the pivot-shift test was the most sensitive for evaluating the stabilizing effect of the ALL in ACL reconstruction. This indicates that gracilis tendon reconstruction of the ALL combined with anatomic single-bundle quadriceps tendon reconstruction of the ACL approaches intact knee kinematics, except at low knee flexion angles.

In our setup, which mirrors the in vivo setting, the results support previous studies regarding the contribution of the ALL to restraining knee laxity in anterior translation and internal rotation, and we here confirm that concurrent ALL and ACL reconstruction can improve knee laxity for patients with severe laxity due to combined ACL and ALL injuries. Previous non-dRSA studies measuring changes in kinematics[43,49,52,57,63,64] or kinetics[45,64] reported a similar relationship between increasing knee flexion angles and increasing ALL effects on internal rotation and anterior translation.

Besides describing a similar effect of the ALL, Schon et al[52] also described excessive constraint of the knee joint after combined ACL and ALL reconstruction. They illustrated a proportional relationship between graft fixation knee flexion angle and overconstraint of the joint. Clinical studies using combined intra- and extra-articular reconstruction techniques have reported deviating results; compared with previous results,[39,41,56] some demonstrated lower ACL graft rupture rates, satisfactory control of

anteroposterior movements, and maintenance of rotational knee laxity without complications such as stiffness or limited range of motion, while others reported high failure rates, poor long-term functional subjective and objective outcomes, and chronic lateral knee pain.[53,69,70] These differences may be attributed to the population/extent of the injury and the surgical reconstruction technique. As described above, the graft fixation knee flexion angle[52] influences knee laxity, but the graft position is also found to influence the ALL length pattern[25,28,30,33,42,67] and thereby knee laxity. These 2 parameters are closely interrelated.

In our study, we used a graft fixation knee flexion angle of approximately 10° to 20° with proximal and posterior femoral graft origins, which did not result in an overconstrained joint below 60°. However, higher flexion angles also need to be investigated because the contribution of the ALL has shown to increase with increasing flexion angles. A review article[38] and a meta-analysis[21] have suggested that lateral extra-articular reinforcement in conjunction with intra-articular reconstruction could be important for controlling rotational knee laxity, and both studies reported a statistically significant reduction in pivot shift in favor of ACL reconstruction combined with extra-articular tenodesis. This could indicate that patient-specific treatment should be considered to a greater extent than is currently the case, especially in light of the distinctness and variations of the ALL position between patients.[9,14,34] Noninvasive methods such as ultrasound[44] and magnetic resonance imaging[19,46,61] may be used for the preoperative evaluation and diagnosis of anterolateral structures such as the ALL.

To our knowledge, the biomechanical influence of the ALL on knee laxity had yet to be investigated in all 6 degrees of freedom. The present study reveals that the ALL supports varus rotation and potentially medial translation. To the best of our knowledge, these effects have not previously been reported. The increase in varus rotation after ALL resection in the ACL-deficient knee was expected because of the anatomic position. However, ACL reconstruction normalized varus rotation. In combination with the observation of no decrease in knee laxity for internal rotation after ACL reconstruction, this indicates that besides anterior-posterior translation, ACL reconstruction in an ACL- and ALL-deficient knee primarily stabilizes varus-valgus rotation. Given the fact that an ALL tear is likely to occur during an ACL tear, this may explain residual laxity and the pivot shift after ACL reconstruction.

For ACL reconstruction as well as combined ACL and ALL reconstruction, a decrease in medial translation to its previous ligament situation without an increase in the resecting ligament stages could indicate overtightening of the ligaments after reconstruction. However, this seems not to be the case because these ligament situations were not significantly different from the intact knee. These kinematic behaviors should be further investigated.

Those patients who experience a residual positive pivot-shift sign after ACL reconstruction may have an unnoticed injury to the lateral aspect of the knee such as the ALL.[8,11] Our results indicate that for patients within this group, combining ACL and ALL reconstruction may outperform traditional procedures because the ALL stabilizes the knee within flexion angles in which laxity is naturally largest without restricting the motion range at higher flexion angles. To confirm our findings, additional clinical research utilizing dynamic methods such as dRSA should be performed comparing rotational laxity of ACL-deficient knees with a positive pivot-shift sign before and after ALL reconstruction.

Our study is not without limitations. Eight specimens may not be sufficient to interpret the results. At sample sizes this small, even random variation across specimens could influence statistical significance; thus, there is a substantial risk of type II errors, in which we failed to reject a false null hypothesis even though a true effect does exist.

The included specimens consisted of pairwise legs from the same donor, which may introduce the potential for heteroscedasticity. However, this was tested and accounted for using the mixed-model statistical method.

Furthermore, our specimens were cadaveric and hence obtained from older patients than those typically undergoing ACL reconstruction.[60] This may have affected our results because age can influence ligament laxity and the fixated strength of ligament reconstruction because of poorer bone quality.[68] Additionally, knee osteoarthritis occurs more commonly in the elderly. Nevertheless, only 1 specimen pair (2 specimens) had osteophytes based on the CT-reconstructed bone models. One case was more severe than the other, but the cartilage was preserved at arthroscopic surgery (International Cartilage Repair Society grade 2).[7] The osteophytes affected the ACS of the femur; thus, the origin was clearly different from the rest of the specimens, as evidenced by a different condylar shape. This resulted in a larger variety of kinematic translation measures at the tibiofemoral joint and caused inevitable interference during the computed rotations. These consequences are seen in the large variation in kinematic movements displayed in Figure 5. However, statistical analysis with and without this specimen did not affect our findings.

The tibial plateau estimation as 1 simple flat plane is a clear limitation when estimating contact points between the femoral and tibial surface models. This may have influenced the lack of clear association between the ligament situations. Hashemi et al[18] found that the posterior tibial slope differs between patients and that the medial and lateral slopes differ within patients. Our general tibial joint surface plane defined by the lateral-medial and anterior-posterior planes may have skewed the contact point calculations during knee flexion. Therefore, we performed a visual inspection to confirm the resemblance between the individual posterior tibial slopes and the applied tibial plateau plane. Unfortunately, it was not possible to correct for medial and lateral plane differences or for the concave shape of the medial and lateral tibial plateaus. However, the method is promising for 2 main reasons. First, it estimates the direct interaction between relevant bones. Second, it is not affected by kinematic calculations of the ACS. Nevertheless, a method that segments the articular cartilage to determine the position and thickness would be beneficial when evaluating bone interaction.

We designed a machine to load the specimens in a manner resembling the pivot-shift test. The final design included controlled internal rotation, followed by a knee flexion movement with high accuracy. It was not possible to fully satisfy the pivot-shift test because we were unable to apply reliable valgus stress during the flexion movement; thus, knee and hip kinematics were completely dependent on internal rotation and flexion movement. However, it could be expected that some valgus stress at the knee was naturally applied because of the forceful internal foot/lower leg rotation. Nevertheless, impingement of the subluxed tibial plateau against the lateral femoral condyle preventing an easy return, as observed in the pivot-shift test, could not be expected with certainty. Some implemented valgus stress in our machine may have resulted in a larger influence of the ALL on knee laxity.[15]

Our instrument design limited the biomechanical evaluation of knee ligaments at large flexion angles (above 60°) because of the confined recording area, but repositioning of the machine could produce knee flexion motions closer to 90°, if needed, at the expense of low flexion angles. Larger recording areas with the dRSA technique may be developed in the future, thus simplifying the recording of clinical motion exercises.

CONCLUSION

This ex vivo study confirms that the ALL is a significant anterolateral stabilizer of the tibiofemoral joint in ACL-deficient knees. Furthermore, this study complements the literature by demonstrating that the ALL affects varus and medial laxity of the knee. Augmented ALL reconstruction with ACL reconstruction significantly improves knee laxity compared with ACL reconstruction alone. The ALL stabilizes the knee at flexion angles in which the ACL has a minor influence. Thus, ALL reconstruction has the potential to improve rotational laxity for patients with a positive pivot-shift sign at the time of repeated or primary ACL reconstruction.

REFERENCES

1. Amis AA, Bull AMJ, Lie DTT. Biomechanics of rotational instability and anatomic anterior cruciate ligament reconstruction. *Oper Tech Orthop*. 2005;15(1):29-35.
2. Anderson AF, Snyder RB, Lipscomb AB Jr. Anterior cruciate ligament reconstruction: a prospective randomized study of three surgical methods. *Am J Sports Med*. 2001;29(3):272-279.
3. Anderst WJ, Tashman S. A method to estimate in vivo dynamic articular surface interaction. *J Biomech*. 2003;36(9):1291-1299.
4. Balasch H, Schiller M, Friebel H, Hoffmann F. Evaluation of anterior knee joint instability with the Rolimeter: a test in comparison with manual assessment and measuring with the KT-1000 arthrometer. *Knee Surg Sports Traumatol Arthrosc*. 1999;7(4):204-208.
5. Bell KM, Rahnemai-Azar AA, Irarrazaval S, et al. In situ force in the anterior cruciate ligament, the lateral collateral ligament, and the anterolateral capsule complex during a simulated pivot shift test. *J Orthop Res*. 2018;36(3):847-853.
6. Benjaminse A, Gokeler A, Van Der Schans CP. Clinical diagnosis of an anterior cruciate ligament rupture: a meta-analysis. *J Orthop Sports Phys Ther*. 2006;36(5):267-288.
7. Brittberg M. Evaluation of cartilage injuries and cartilage repair. *Osteologie*. 2000;9(1):17-25.
8. Campos JC, Chung CB, Lektrakul N, et al. Pathogenesis of the Segond fracture: anatomic and MR imaging evidence of an iliotibial tract or anterior oblique band avulsion. *Radiology*. 2001;219(2):381-386.
9. Caterine S, Litchfield R, Johnson M, Chronik B, Getgood A. A cadaveric study of the anterolateral ligament: re-introducing the lateral capsular ligament. *Knee Surg Sports Traumatol Arthrosc*. 2015;23(11):3186-3195.
10. Claes S, Luyckx T, Vereecke E, Bellemans J. The Segond fracture: a bony injury of the anterolateral ligament of the knee. *Arthroscopy*. 2013;30(11):1475-1482.
11. De Maeseneer M, Boulet C, Willekens I, et al. Segond fracture: involvement of the iliotibial band, anterolateral ligament, and anterior arm of the biceps femoris in knee trauma. *Skeletal Radiol*. 2014;44(3):413-421.
12. de Raedt S, Mechlenburg I, Stilling M, Rømer L, Søballe K, de Bruijne M. Automated measurement of diagnostic angles for hip dysplasia. In: *SPIE Medical Imaging 2013*. Lake Buena Vista, FL: SPIE; 2013. doi:10.1117/12.2007599.
13. Dodds AL, Gupte CM, Neyret P, Williams AM, Amis AA. Extra-articular techniques in anterior cruciate ligament reconstruction: a literature review. *J Bone Joint Surg Br*. 2011;93-B(11):1440-1448.
14. Dodds AL, Halewood C, Gupte CM, Williams A, Amis AA. The anterolateral ligament: anatomy, length changes and association with the Segond fracture. *Bone Joint J*. 2014;96B(3):325-331.
15. Engebretsen L, Wijdicks CA, Anderson CJ, Westerhaus B, LaPrade RF. Evaluation of a simulated pivot shift test: a biomechanical study. *Knee Surg Sports Traumatol Arthrosc*. 2012;20(4):698-702.
16. Galway HR, MacIntosh DL. The lateral pivot shift: a symptom and sign of anterior cruciate ligament insufficiency. *Clin Orthop Relat Res*. 1980;(147):45-50.
17. Grood ES, Suntay WJ. A joint coordinate system for the clinical description of three-dimensional motions: application to the knee. *J Biomech Eng*. 1983;105(2):136-144.
18. Hashemi J, Chandrashekar N, Gill B, et al. The geometry of the tibial plateau and its influence on the biomechanics of the tibiofemoral joint. *J Bone Joint Surg Am*. 2008;90(12):2724-2734.
19. Helito CP, Demange MK, Helito PVP, et al. Evaluation of the anterolateral ligament of the knee by means of magnetic resonance examination. *Rev Bras Ortop*. 2015;50(2):214-219.
20. Helito CP, Helito PVP, Bonadio MB, et al. Evaluation of the length and isometric pattern of the anterolateral ligament with serial computer tomography. *Orthop J Sports Med*. 2014;2(12):2325967114562205.
21. Hewison CE, Tran MN, Kaniki N, Remtulla A, Bryant D, Getgood AM. Lateral extra-articular tenodesis reduces rotational laxity when combined with anterior cruciate ligament reconstruction: a systematic review of the literature. *Arthroscopy*. 2015;31(10):2022-2034.
22. Hoshino Y, Tashman S. Internal tibial rotation during in vivo, dynamic activity induces greater sliding of tibio-femoral joint contact on the medial compartment. *Knee Surg Sports Traumatol Arthrosc*. 2012;20(7):1268-1275.
23. Houck J, Lerner A, Gushue D, Yack HJ. Self-reported giving-way episode during a stepping-down task: case report of a subject with an ACL-deficient knee. *J Orthop Sports Phys Ther*. 2003;33(5):273-282.
24. Houck J, Yack HJ. Giving way event during a combined stepping and crossover cutting task in an individual with anterior cruciate ligament deficiency. *J Orthop Sports Phys Ther*. 2001;31(9):481-485.
25. Imbert P, Lutz C, Daggett M, et al. Isometric characteristics of the anterolateral ligament of the knee: a cadaveric navigation study. *Arthroscopy*. 2016;32(10):2017-2024.
26. James EW, LaPrade CM, LaPrade RF. Anatomy and biomechanics of the lateral side of the knee and surgical implications. *Sports Med Arthrosc*. 2015;23(1):2-9.
27. Kaptein BL, Valstar ER, Stoel BC, Rozing PM, Reiber JHC. Evaluation of three pose estimation algorithms for model-based roentgen

stereophotogrammetric analysis. *Proc Inst Mech Eng H*. 2004;218(4): 231-238.
28. Katakura M, Koga H, Nakamura K, Sekiya I, Muneta T. Effects of different femoral tunnel positions on tension changes in anterolateral ligament reconstruction. *Knee Surg Sports Traumatol Arthrosc*. 2017; 25(4):1272-1278.
29. Kennedy MI, Claes S, Fuso FAF, et al. The anterolateral ligament: an anatomic, radiographic, and biomechanical analysis. *Am J Sports Med*. 2015;43(7):1606-1615.
30. Kernkamp WA, Van de Velde SK, Hosseini A, et al. In vivo anterolateral ligament length change in the healthy knee during functional activities: a combined magnetic resonance and dual fluoroscopic imaging analysis. *Arthroscopy*. 2017;33(1):133-139.
31. Kerr HD. Segond fracture, hemarthrosis, and anterior cruciate ligament disruption. *J Emerg Med*. 1990;8(1):29-33.
32. Kittl C, El-Daou H, Athwal KK, et al. The role of the anterolateral structures and the ACL in controlling laxity of the intact and ACL-deficient knee. *Am J Sports Med*. 2015;44(2):345-354.
33. Kittl C, Halewood C, Stephen JM, et al. Length change patterns in the lateral extra-articular structures of the knee and related reconstructions. *Am J Sports Med*. 2015;43(2):354-362.
34. Kosy JD, Soni A, Venkatesh R, Mandalia VI. The anterolateral ligament of the knee: unwrapping the enigma. Anatomical study and comparison to previous reports. *J Orthop Traumatol*. 2016;17(4): 303-308.
35. Krčah M, Székely G, Blanc R. Fully automatic and fast segmentation of the femur bone from 3D-CT images with no shape prior. In: *2011 IEEE International Symposium on Biomedical Imaging: From Nano to Macro*. Chicago, IL: IEEE; 2011. doi:10.1109/ISBI.2011.5872823.
36. Kujala UM, Nelimarkka O, Koskinen SK. Relationship between the pivot shift and the configuration of the lateral tibial plateau. *Arch Orthop Trauma Surg*. 1992;111(4):228-229.
37. Lohmander LS, Englund PM, Dahl LL, Roos EM. The long-term consequence of anterior cruciate ligament and meniscus injuries: osteoarthritis. *Am J Sports Med*. 2007;35(10):1756-1769.
38. Lording TD, Lustig S, Servien E, Neyret P. Lateral reinforcement in anterior cruciate ligament reconstruction. *Asia Pac J Sports Med Arthrosc Rehabil Technol*. 2014;1:3-10.
39. Marcacci M, Zaffagnini S, Giordano G, Iacono F, Presti ML. Anterior cruciate ligament reconstruction associated with extra-articular tenodesis: a prospective clinical and radiographic evaluation with 10- to 13-year follow-up. *Am J Sports Med*. 2009;37(4):707-714.
40. Miranda DL, Rainbow MJ, Leventhal EL, Crisco JJ, Fleming BC. Automatic determination of anatomical coordinate systems for three-dimensional bone models of the isolated human knee. *J Biomech*. 2010;43(8):1623-1626.
41. Monaco E, Ferretti A, Labianca L, et al. Navigated knee kinematics after cutting of the ACL and its secondary restraint. *Knee Surg Sports Traumatol Arthrosc*. 2012;20(5):870-877.
42. Neri T, Palpacuer F, Testa R, et al. The anterolateral ligament: anatomic implications for its reconstruction. *Knee*. 2017;24(5):1083-1089.
43. Nitri M, Rasmussen MT, Williams BT, et al. An in vitro robotic assessment of the anterolateral ligament, part 2: anterolateral ligament reconstruction combined with anterior cruciate ligament reconstruction. *Am J Sports Med*. 2016;44(3):593-601.
44. Oshima T, Nakase J, Numata H, Takata Y, Tsuchiya H. Ultrasonography imaging of the anterolateral ligament using real-time virtual sonography. *Knee*. 2016;23(2):198-202.
45. Parsons EM, Gee AO, Spiekerman C, Cavanagh PR. The biomechanical function of the anterolateral ligament of the knee. *Am J Sports Med*. 2015;43(3):669-674.
46. Patel KA, Chhabra A, Goodwin JA, Hartigan DE. Identification of the anterolateral ligament on magnetic resonance imaging. *Arthrosc Tech*. 2017;6(1):e137-e141.
47. Pomajzl R, Maerz T, Shams C, Guettler J, Bicos J. A review of the anterolateral ligament of the knee: current knowledge regarding its incidence, anatomy, biomechanics, and surgical dissection. *Arthroscopy*. 2014;31(3):583-591.
48. Prins AH, Kaptein BL, Stoel BC, Lahaye DJP, Valstar ER. Performance of local optimization in single-plane fluoroscopic analysis for total knee arthroplasty. *J Biomech*. 2015;48(14):3837-3845.
49. Rasmussen MT, Nitri M, Williams BT, et al. An in vitro robotic assessment of the anterolateral ligament, part 1: secondary role of the anterolateral ligament in the setting of an anterior cruciate ligament injury. *Am J Sports Med*. 2016;44(3):585-592.
50. Ristanis S, Giakas G, Papageorgiou CD, Moraiti T, Stergiou N, Georgoulis AD. The effects of anterior cruciate ligament reconstruction on tibial rotation during pivoting after descending stairs. *Knee Surg Sports Traumatol Arthrosc*. 2003;11(6):360-365.
51. Schindler OS. Surgery for anterior cruciate ligament deficiency: a historical perspective. *Knee Surg Sports Traumatol Arthrosc*. 2012; 20(1):5-47.
52. Schon JM, Moatshe G, Brady AW, et al. Anatomic anterolateral ligament reconstruction of the knee leads to overconstraint at any fixation angle. *Am J Sports Med*. 2016;44(10):2546-2556.
53. Sgaglione NA, Warren RF, Wickiewicz TL, Gold DA, Panariello RA. Primary repair with semitendinosus tendon augmentation of acute anterior cruciate ligament injuries. *Am J Sports Med*. 1990;18(1): 64-73.
54. Siebold R, Schuhmacher P, Fernandez F, et al. Flat midsubstance of the anterior cruciate ligament with tibial "C"-shaped insertion site. *Knee Surg Sports Traumatol Arthrosc*. 2014;23(11):3136-3142.
55. Śmigielski R, Zdanowicz U, Drwięga M, Ciszek B, Ciszkowska-Łysoń B, Siebold R. Ribbon like appearance of the midsubstance fibres of the anterior cruciate ligament close to its femoral insertion site: a cadaveric study including 111 knees. *Knee Surg Sports Traumatol Arthrosc*. 2014;23(11):3143-3150.
56. Sonnery-Cottet B, Thaunat M, Freychet B, Pupim BHB, Murphy CG, Claes S. Outcome of a combined anterior cruciate ligament and anterolateral ligament reconstruction technique with a minimum 2-year follow-up. *Am J Sports Med*. 2015;43(7):1598-1605.
57. Spencer L, Burkhart TA, Tran MN, et al. Biomechanical analysis of simulated clinical testing and reconstruction of the anterolateral ligament of the knee. *Am J Sports Med*. 2015;43(9):2189-2197.
58. Stentz-Olesen K, Nielsen ET, De Raedt S, et al. Validation of static and dynamic radiostereometric analysis of the knee joint using bone models from CT data. *Bone Joint Res*. 2017;6(6):376-384.
59. Stergiou N, Ristanis S. Tibial rotation in anterior cruciate ligament (ACL)-deficient and ACL-reconstructed knees. *Sports Med*. 2007; 37(7):601-613.
60. Styregruppen for DKRR. Dansk Korsbånds Rekonstruktions Register Årsrapport 2015. Available at: https://www.sundhed.dk/content/cms/0/4700_dkrr_aarsrapport_2016.pdf. Accessed August 1, 2016.
61. Taneja AK, Miranda FC, Braga CAP, et al. MRI features of the anterolateral ligament of the knee. *Skeletal Radiol*. 2014;44(3):403-410.
62. Tashman S, Collon D, Anderson K, Kolowich P, Anderst W. Abnormal rotational knee motion during running after anterior cruciate ligament reconstruction. *Am J Sports Med*. 2004;32(4):975-983.
63. Tavlo M, Eljaja S, Jensen JT, Siersma VD, Krogsgaard MR. The role of the anterolateral ligament in ACL insufficient and reconstructed knees on rotatory stability: a biomechanical study on human cadavers. *Scand J Med Sci Sports*. 2016;26(8):960-966.
64. Thein R, Boorman-Padgett J, Stone K, Wickiewicz TL, Imhauser CW, Pearle AD. Biomechanical assessment of the anterolateral ligament of the knee: a secondary restraint in simulated tests of the pivot shift and of anterior stability. *J Bone Joint Surg Am*. 2016; 98(11):937-943.
65. Torg JS, Conrad W, Kalen V. Clinical diagnosis of anterior cruciate ligament instability in the athlete. *Am J Sports Med*. 1976;4(2):84-93.
66. Van Der Watt L, Khan M, Rothrauff BB, et al. The structure and function of the anterolateral ligament of the knee: a systematic review. *Arthroscopy*. 2015;31(3):569-582.
67. Van de Velde SK, Kernkamp WA, Hosseini A, LaPrade RF, van Arkel ER, Li G. In vivo length changes of the anterolateral ligament and related extra-articular reconstructions. *Am J Sports Med*. 2016; 44(10):2557-2562.

68. Wang X, Shen X, Li X, Agrawal CM. Age-related changes in the collagen network and toughness of bone. *Bone*. 2002;31(1):1-7.
69. Yamaguchi S, Sasho T, Tsuchiya A, Wada Y, Moriya H. Long term results of anterior cruciate ligament reconstruction with iliotibial tract: 6-, 13-, and 24-year longitudinal follow-up. *Knee Surg Sports Traumatol Arthrosc*. 2006;14(11):1094-1100.
70. Zaffagnini S, Bruni D, Russo A, et al. ST/G ACL reconstruction: double strand plus extra-articular sling vs double bundle, randomized study at 3-year follow-up. *Scand J Med Sci Sports*. 2008;18(5):573-581.
71. Zens M, Niemeyer P, Ruhhammer J, et al. Length changes of the anterolateral ligament during passive knee motion: a human cadaveric study. *Am J Sports Med*. 2015;43(10):2545-2552.